Constraining absolute deformation ages: the relationship between deformation mechanisms and isotope systematics

Steven M. Reddy [a],*, Graham J. Potts [b]

[a]*Tectonics Special Research Centre, School of Applied Geology, Curtin University of Technology, Perth, WA 6102, Australia*
[b]*Department of Earth Sciences, University of Liverpool, Liverpool L69 3BX, UK*

Abstract

Isotope diffusion in a mineral is strongly temperature dependent but is also a function of grain size. Deformation must, therefore, be an important consideration in the interpretation of isotopic data because it provides a means of modifying grain size and shape. We illustrate the range of different deformation mechanisms common in micas and use simple models to investigate the relationship between these and isotope diffusion. We consider three different thermal scenarios with deformation taking place during: (a) the prograde heating path, (b) at the closure temperature of the deforming mineral, and (c) at temperatures significantly below the closure temperature. We have modelled these simple systems using a finite difference algorithm that simulates argon diffusion profiles and bulk ages. This modelling illustrates that obtaining deformation ages is critically dependent on an understanding and recognition of the different deformation mechanisms that have affected the sample. In the cases where deformation causes a change in grain size, it is important to characterise both the temperature at which deformation takes place and the closure temperature of grains formed during the deformation. The development of grains with T_c greater than the deformation temperature may record a deformation age. Examples of this condition include: (i) neocrystallisation; (ii) grain size reduction occurring at temperatures below T_c (of the reduced grain size) where the deformation mechanism has reset the grains; and (iii) deformation-induced grain coarsening. © 1999 Elsevier Science Ltd. All rights reserved.

1. Introduction

The absolute ages of individual deformation events are fundamental to our understanding of the rates of deformation processes and tectonic histories. Radiometric-dating techniques have been employed in attempts to determine absolute ages of deformation (e.g. Kligfield et al., 1986; Kralik et al., 1987; Kelley, 1988; Thoni, 1988; Dunlap et al., 1991; Kelley et al., 1994; Freeman et al., 1997; Reddy et al., 1999a). However, in deformed materials, isotope systematics are usually difficult to interpret because isotope migration and the alteration or resetting of isotope systems may be a function of both deformation and temperature. It is our belief that the interpretation of

radiometric data as true deformation ages may often be erroneous. This stems from over-simplification of both the microstructural history of the samples (frequently the term 'recrystallisation' is used without any concern for the mechanisms) and the diffusion models employed. In this contribution we discuss the effects that different deformation mechanisms may have on isotope systematics and illustrate some of the implications for radiometric dating using a series of simple models. Many geochronologists have already considered the relationship between temperature and grain size and used this to constrain thermal histories of metamorphic rocks. Here, by applying recent advances in our understanding of mica deformation mechanisms and isotope systems, we extend this work to consider cases in which grain size changes as a result of deformation (e.g. Kelley, 1988; Goodwin and Renne, 1991; Reddy et al., 1996). Our aim is to illustrate some of the potential complexities associated with dating defor-

---

* Corresponding author.

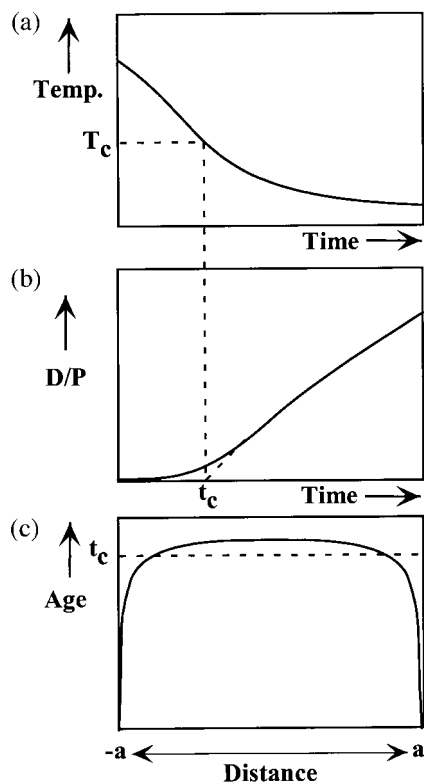*E-mail address:* sreddy@lithos.curtin.edu.au (Steven M. Reddy)

Fig. 1. (a) Temperature (*T*)–time (*t*) path for a simple cooling system. (b) Change in daughter/parent (D/P) ratio of a radiogenic isotopic system as a function of time. Together parts (a) and (b) illustrate the relationship between apparent age (t_c) and closure temperature (T_c) (after Dodson, 1973). (c) Schematic diagram of the distribution of apparent ages in an individual grain of radius *a* (after Dodson, 1986). The age profile arises from the diffusion of argon from the grain. The dotted line represents the spatially averaged age of the grain, which is equivalent to t_c in part (b).

mation and provide the structural geologist with a framework within which published 'absolute' deformation ages may be critically assessed.

We restrict our discussion to the $^{40}Ar/^{39}Ar$ dating technique. We do this because it is the isotopic system with which we have most experience with regard to deformation studies (Kelley et al., 1994; Reddy et al., 1996, 1997, 1999b; Pickles et al., 1997). We have placed emphasis on the behaviour of argon in micas. Our reasons for this are that micas are a common K-bearing phase in many deformed crustal rocks; they are widely dated by several isotopic techniques and they appear mineralogically and isotopically less complicated than many other K-bearing phases (e.g. K-feldspar). Micas have the added advantage that as major phases their microstructures can be often related to deformation at the larger scale, something that is difficult to achieve with accessory mineral phases. In addition, the application of $^{40}Ar/^{39}Ar$ dating of white mica and biotite to constrain deformation ages has been attempted numerous times (Kligfield et al., 1986;

Wijbrans and McDougall, 1986; Kelley, 1988; Dunlap et al., 1991; Goodwin and Renne, 1991; West and Lux, 1993; Kelley et al., 1994; Kirschner et al., 1996; Reddy et al., 1996; Dunlap, 1997). Although we restrict our analysis to micas and a specific isotope system, our conclusions are general and will be applicable to other isotopic and mineral systems.

2. Diffusion and isotopic ages

In the absence of fluid advection, the migration of isotopic species is driven by diffusion. Within individual grains, this is due to concentration gradients within grains and at their boundaries. Diffusion is a strongly temperature-dependent process governed by an Arrhenius relationship. The extent of diffusive equilibration in a mineral is also related to the grain size; the smaller the diffusion distance the shorter the time taken for material to travel from core to rim. Deformation must, therefore, be an important consideration in the interpretation of isotopic data because it provides a means of changing grain size and therefore affecting isotope systematics.

The relationship between diffusion, temperature and grain size in geological materials was initially developed in terms of the mathematical approximation known as 'closure temperature' (T_c). The T_c of a mineral is defined as its temperature at a time corresponding to its apparent age (Dodson, 1973; Fig. 1), and it relates to a temperature below which significant daughter isotopes accumulate in the mineral. It should be emphasised that T_c does *not* represent the temperature below which there is no diffusion. It is a mathematical simplification that relates the mean age of the age profile across a grain to a temperature in the cooling history of a mineral for a simple cooling system (Dodson, 1986; Fig. 1). In most cases, diffusion below T_c will be insignificant. However, in coarse-grained minerals over several millimetres in diameter, diffusion below T_c can significantly modify calculated apparent ages because of the scale and magnitude of isotopic diffusion (Reddy et al., 1996). The closure temperature model is based on several significant assumptions, some of which may not be valid in many situations. Of these, isotope migration being dominated by a volume diffusion process (cf. Lee, 1995) and the concentration of diffusing species in the grain boundary network being zero (cf. Reddy et al., 1997) are possibly the most significant. Therefore, there are potential problems and pitfalls associated with the application of the closure temperature model. However, we use T_c throughout this paper as it represents a useful and readily calculable reference temperature below which, the rate of isotope diffusion rapidly decreases.

Closure temperature is controlled by a number of
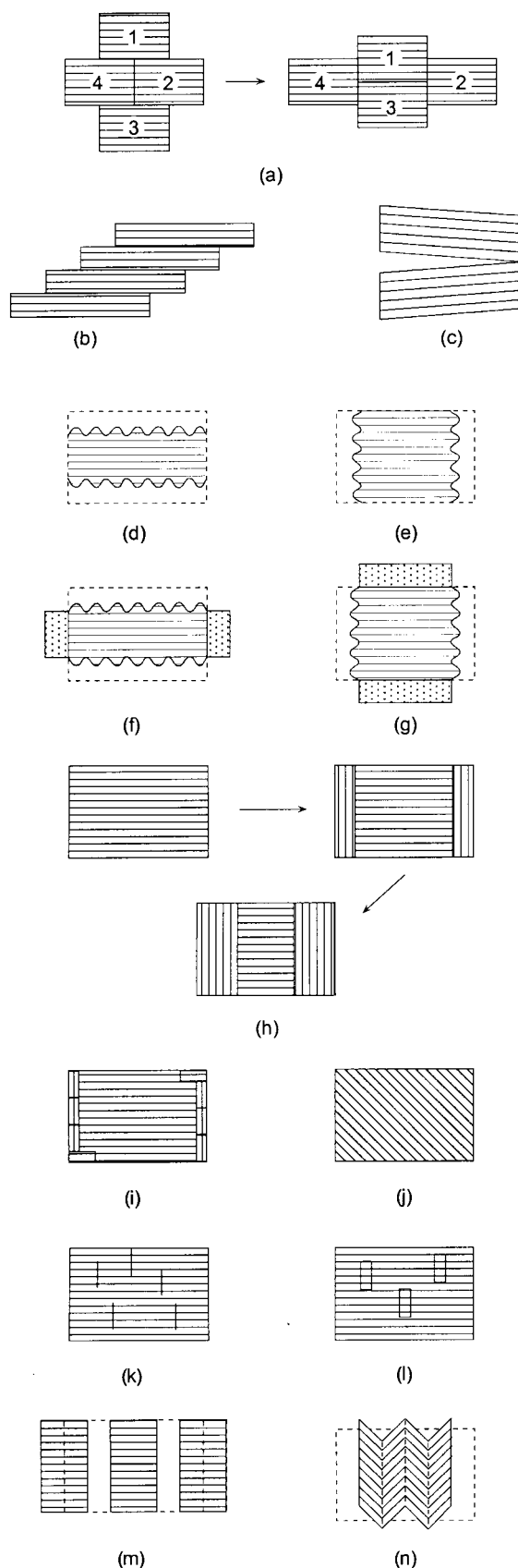
intrinsic parameters and externally controlled variables. Values of T_c depend on the diffusion parameters for the isotopic species of concern and the mineral in which diffusion is taking place. Sample cooling rate will affect T_c with faster cooling rates yielding higher values for T_c. Grain size also has a strong control on T_c (Dodson, 1973; Hames and Bowring, 1994). As deformation has the potential for significantly modifying grain size, deformation processes may significantly change mineral closure temperatures and therefore the isotopic ages we obtain in the laboratory. Furthermore, argon diffusion in micas may be 1000 times greater parallel to (001) planes than perpendicular to them (e.g. Giletti, 1974). As a consequence, argon diffusion in micas is normally modelled in terms of cylindrical diffusion geometry (Hames and Bowring, 1994). Therefore, when considering the relationship between argon diffusion and deformation in micas it is also necessary to consider whether or not a particular deformation mechanism changes grain size parallel to (001) planes and/or perpendicular to them. These relationships are considered further in the following sections. First we describe how different deformation mechanisms may modify the grain size of micas. Then we assess how these changes may influence the interpretation of argon isotopic ages of white micas in terms of cooling or deformation ages.

Fig. 2. Conceptual models of grain-scale deformation mechanisms in micas. (a) Grain boundary sliding. (b) Sliding on basal (001) planes with or without fracture. (c) Cleavage fracture along basal planes. Although grain size is reduced, the higher diffusion rate parallel to (001) ensures that the effective grain size is unchanged by mechanisms (b) and (c). (d) Diffusive mass transfer in an open system that leads to a reduction in grain volume. Dissolution parallel to (001) does not significantly change the effective grain size for argon diffusion. (e) Diffusive mass transfer in an open system. Dissolution perpendicular to the basal planes may significantly reduce the effective grain size. (f)–(g) Diffusive mass transfer in a closed system produces changes in effective grain size of relict grains [as described in (d) and (e)]. Overgrowths will consist of new material that did not possess radiogenic argon at the time of growth. In (f) the overgrowths increase the effective grain size but in (g) they have little or no effect. (h) Internal grain boundary migration recrystallisation. The new grain boundaries grow at a high angle to the (001) planes of the host. (i) Grain boundary migration recrystallisation. In this case new small grains are formed at the margins of the porphyroclast. (j) Grain boundary recrystallisation may result in complete recrystallisation where, although the grain may not significantly change size (and shape) the recrystallisation process may change the effective grain size [parallel to (001)] and expel argon from the grain. (k) Discontinuities at high angles to (001) planes in micas. The discontinuities may be dislocation walls, fractures or a combination of both. (l) Subgrains in micas. These are not common and appear to be dispersed throughout the grains unlike more familiar microstructures in quartz. (m) Fracture perpendicular or at moderate angles to (001) planes. (n) Kinking. The axial surfaces of the kinks may behave as grain boundaries and thus, the grain size is reduced. Note that recrystallisation of new small grains may occur along the (highly deformed) kink band axial surfaces.

3. Deformation mechanisms and isotope diffusion

The deformation of micas has been studied in both naturally deformed samples (Eisbacher, 1970; Etheridge and Hobbs, 1974; Cosgrove, 1976; Wilson and Bell, 1979; Bell and Wilson, 1981; Bell and Rubenach, 1983; Behrmann, 1984; Lister and Snoke, 1984; Bell et al., 1986; Gibson, 1990; Goodwin and Wenk, 1990; Kanaori et al., 1991; Li et al., 1994; Worley et al., 1997) and experimentally (Etheridge and Hobbs, 1974; Meike, 1989; Kronenberg et al., 1990; Shea and Kronenberg, 1992, 1993; Christofferson and Kronenberg, 1993; Mares and Kronenberg, 1993). These studies indicate that mica deformation is strongly anisotropic and dominated by dislocation glide parallel to (001) and kinking. However, other mechanisms may also occur and these have implications for isotope systematics.

Grain boundary sliding usually takes place at high temperatures and is enhanced by diffusive mass transfer processes. It is usually restricted to fine-grained rocks and is a common deformation mechanism in fault zones (Gibson, 1990). Strain may be accommodated with little internal deformation of grains and with no change in grain size (Fig. 2a). Similarly, slip along mica cleavages (Fig. 2b; Wilson and Bell, 1979; Bell and Wilson, 1981; Behrmann, 1984; Bell et al., 1986; Goodwin and Wenk, 1990; Kanaori et al., 1991; Shea and Kronenberg, 1992, 1993; Christofferson and Kronenberg, 1993; Mares and Kronenberg, 1993) and cleavage fracture processes (Fig. 2c; Behrmann, 1984; Lister and Snoke, 1984; Kanaori et al., 1991; Shea and Kronenberg, 1992) may also accommodate strain without a change in effective grain size. Since these deformation mechanisms do not result in a change in effective grain size they do not modify the closure temperature of the grains.

Diffusion-accommodated deformation mechanisms of silicates (Cosgrove, 1976; Wilson and Bell, 1979; Lister and Snoke, 1984; Gibson, 1990; Li et al., 1994; Worley et al., 1997) may affect grain size in a number of different ways. The diffusion of material in an open system leads to a reduction in grain volume. If, as is the case in mica, the mineral concerned has a non-spherical diffusion geometry for argon (Giletti, 1974; Hames and Bowring, 1994) then the grain volume may change while the effective grain radius for argon diffusion remains constant (Fig. 2d). If removal of mica takes place perpendicular to (001) (Fig. 2e) then the effective grain radius will be reduced and consequently T_c will be modified. When diffusive mass transfer takes place within a closed system, grain volumes may remain constant but the sites of dissolution and precipitation in micas will allow both increase (Fig. 2f) and decrease (Fig. 2g) in effective grain size. The sites of dissolution and precipitation will be dependent upon the orientation of the individual grains relative to the stress field. Therefore, it is likely that the effective grain size of the grain for isotopic diffusion will also be orientation dependent for individual grains. The dissolution step of the diffusive mass transfer process may also remove material that had an original radiogenic argon component and replace it with material of no finite age. Therefore, diffusive mass transfer mechanisms have the potential to reset or alter isotope systems.

During the development of so-called 'mica-fish', internal grain boundary migration recrystallisation may occur where the ends of the grain become isolated by the growth of new grain boundaries (Fig. 2h; Eisbacher, 1970; Lister and Snoke, 1984; Gibson, 1990). As deformation proceeds the new boundaries may migrate inwards reducing the grain size of the porphyroclast still further (Fig. 2h; Lister and Snoke, 1984). Thus, this form of recrystallisation results in marked grain size reduction and although the ends grow, it is at the expense of the original grain. Similarly, large numbers of small grains may grow around the edges of the porphyroclast (Fig. 2i; Lister and Snoke, 1984). In such cases, the grain size reduction of the host is not as great but the new grains have much smaller sizes in comparison to grain boundary migration recrystallisation (Fig. 2h). These mechanisms are important in isotopic studies because they produce marked changes in grain size and closure temperature. These mechanisms may lead to complete recrystallisation where the grain almost retains its original shape but the orientation of the (001) planes is changed (Fig. 2j; Etheridge and Hobbs, 1974; Lister and Snoke, 1984). Although this does not necessarily lead to grain size reduction the recrystallisation process may expel argon and isotopically reset the grain.

Dislocation-accommodated deformation mechanisms may have a complex effect on isotope systematics. At a fundamental level, diffusion of isotopes along dislocations is significantly faster than volume diffusion (Lee and Aldama, 1992; Lee, 1995). Dislocation migration through mineral lattices may also sweep along inert gases such that argon migration is related to the migration rate of dislocations and therefore stress and strain rate. These complexities are beyond the scope of this paper and we only consider the results of dislocation-accommodated deformation mechanisms in terms of grain size variations.

Several authors have reported the presence of discontinuities at a high angle to the (001) planes in micas (Fig. 2k). Wilson and Bell (1979) and Bell and Wilson (1981) described the segmentation of biotite and, using transmission electron microscopy, Shea and Kronenberg (1992, 1993) and Christofferson and Kronenberg (1993) were able to demonstrate that the pile up of dislocations could produce dislocation walls

in biotite. Shea and Kronenberg (1993) also noted that these walls were occasionally fractured and discontinuous fractures have been found in white micas (Bell and Wilson, 1981) and biotite (Wilson and Bell, 1979; Bell and Wilson, 1981). It is difficult to evaluate the effects of these microstructures; they may enhance the diffusion of argon at right angles to the (001) but if the discontinuities terminate within the grain they may have little or no effect. However, if they form a connected network they may reduce the effective grain size by providing fast diffusion pathways (Lee and Aldama, 1992; Lee, 1995).

The production of subgrains (Fig. 2l; Bell and Wilson, 1981) and continued rotation of subgrain walls by the addition of dislocation networks may result in a grain size reduction during deformation. However, the extent of subgrain rotation recrystallisation in micas is not well known. Studies of naturally deformed micas have recognised subgrain development in micas at high metamorphic grades (Bell, 1979). In contrast, experimental deformation studies have failed to show evidence for dislocation climb as a mechanism in micas (e.g. Kronenberg et al., 1990; Mares and Kronenberg, 1993) but this may simply reflect laboratory conditions. The small number of relatively dispersed subgrains observed in published studies suggests that this deformation mechanism may have little or no significant effect on mica argon ages.

The cataclastic deformation of mica will lead to grain size reduction. However, due to the marked diffusional anisotropy of white mica, we have drawn a distinction between cleavage fracture processes (Fig. 2c) and fracturing perpendicular or at a high angle to (001) (Fig. 2m). In the latter case the fractures may be the result of crack propagation (Mares and Kronenberg, 1993) or grain boudinage (Wilson and Bell, 1979; Behrmann, 1984; Lister and Snoke, 1984) and produce a greatly reduced grain size. Thus, these processes may significantly reduce T_c.

In addition to the above deformation mechanisms, deformation may also lead to the nucleation and crystallisation of new mineral grains. Neocrystallisation of micas during deformation is widely recognised (Bell, 1979; Behrmann, 1984; Lister and Snoke, 1984) and is an important process in argon dating because such grains should contain no radiogenic isotope component at the time of deformation.

A common but complex microstructure in deformed micas is kinking (Fig. 2k; Etheridge and Hobbs, 1974; Cosgrove, 1976; Wilson and Bell, 1979; Bell and Wilson, 1981; Bell and Rubenach, 1983; Lister and Snoke, 1984; Bell et al., 1986; Gibson, 1990; Kanaori et al., 1991; Shea and Kronenberg, 1992, 1993; Mares and Kronenberg, 1993; Li et al., 1994). The maximum grain size in kinked micas will be dependent upon the half-wavelength of the kink structure. However, the

minimum grain size associated with kink band boundaries will be controlled by grain boundary migration, diffusive mass transfer, fracture mechanisms and possibly subgrain rotation recrystallisation taking place in the kink band boundary (e.g. Bell et al., 1986). The interactions of this range of mechanisms would be expected to significantly affect argon isotope systematics around kink bands. High spatial resolution argon dating from around such microstructures appears to confirm this (Reddy et al., 1996). In the simplest case, kinking will lead to a general decrease in T_c throughout the deformed grains and the distribution of variations in T_c will be related to strain variations in the deformed grains. As kinking is directly linked to slip on (001), the formation of kink bands is also strongly orientation dependent. There is likely to be an orientation dependence on T_c and, therefore, on preserved isotopic ages.

The above discussion outlines some of the characteristics that particular deformation mechanisms possess and in particular illustrates the potential for the different mechanisms to modify grain sizes in deforming micas in different ways. As grain size is an important control on T_c, then it is clear that some deformation mechanisms will have a significant effect on isotope systematics while others will not. However, the significance of the different deformation mechanisms will be dependent upon the temperature at which the deformation takes place, the closure temperature of the original grains and the modification of the closure temperature by the deformation process. The effects of these factors are discussed in the following section.

4. Relationship of deformation, diffusion and thermal history

In this section, we discuss the potential importance of deformation–isotope diffusion relationships by considering the timing of deformation in relation to the thermal history of a set of model samples. In these models we only consider volume diffusion in white mica [diffusion parameters from Hames and Bowring (1994)]. In all cases, we have assumed a pre-deformational grain radius of 1 mm and, where relevant, a grain radius reduction to 0.1 mm. The effects of grain coarsening are also described qualitatively based on these results. Throughout we assume a 10°C/Ma cooling rate. These values yield T_c of 445°C and 368°C for 1 mm and 0.1 mm grains, respectively. We discuss a very simple system comprising a metamorphic event in which three deformation events have taken place. The three events (D_1, D_2 and D_3) represent short-lived periods of deformation that occurred at the following times: (1) during the prograde temperature–time (T–t) path (450°C); (2) around T_c during cooling (445°C);

and (3) at temperatures significantly below T_c for the 1 mm grains (395°C) (Fig. 3). In the case of D_1, we have modelled a 10°C/Ma heating rate up to the metamorphic peak at 500°C and the metamorphic peak temperature was maintained for 5 Ma before the commencement of cooling. We first consider deformations that have no effect on the grain size of white micas in the sample. Later, we use these results to consider the effects of progressively more complicated cases with deformation-induced, grain size changes. We have modelled these simple systems using a finite difference algorithm that simulates argon diffusion profiles and bulk ages [the DIFFARG program of Wheeler (1996)].

4.1. Deformation with no change in grain size

In this simple case, deformation of the rock is modelled assuming that deformation does not result in a change in grain size. We do not necessarily believe that such simple cases commonly occur in nature. However, the examples illustrate some of the complexities that arise even in the simplest systems. The deformation mechanisms being modelled include those in which there is no internal deformation (e.g. grain boundary sliding, Fig. 2a) and those in which intra-grain deformation does take place (e.g. cleavage slip, cleavage fracture and diffusional mass transfer perpendicular to (001); Fig. 2b, c and d).

In our first example, the effect of the post-deformational thermal history has been modelled following the D_1 deformation. The spatial distribution of radiogenic argon in the grain is shown in Fig. 4a(i), the apparent or spatially averaged age across a single grain is shown in Fig. 4a(ii) and the temperature time path after deformation (at $t = 0$) is shown in Fig. 4a(iii). Since the deformation does not modify the effective grain size, the final distribution of ages would be the same as if the grains had not undergone the deformation event.
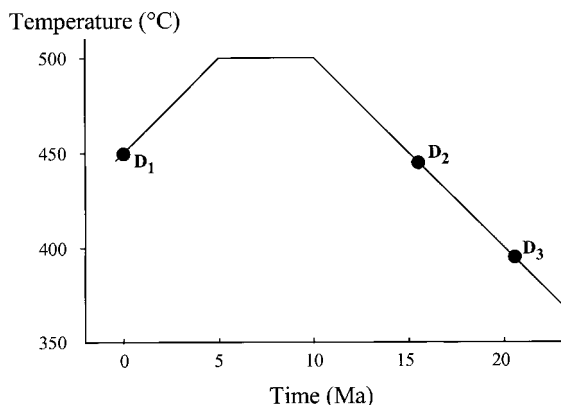

Fig. 3. Illustration of the relationship between thermal history and deformation events used to investigate the association between deformation mechanisms and argon diffusion.

The final age recorded by the sample, 30 Ma after the deformation event, is 15 Ma. This age corresponds (within 0.5 Ma) to the time at which the rock passed through the 445°C closure temperature on the retrograde side of the T–t path. Thus there is no record of the deformation event preserved in the grains because the temperature was sufficiently high that radiogenic argon was lost from the sample. However, an interesting feature highlighted by the modelling [Fig. 4a(i–iii)] is that at the metamorphic peak (c. 50°C above the closure temperature), the grain still has a finite age (c. 1 Ma) due to the mismatch in the relative rates of radiogenic argon production and loss by diffusion.

For D_2, deformation takes place at T_c. However, because there is no change in grain size (Fig. 2a) or effective grain size (Fig. 2b and c), the final age will be identical to that above and the grain will yield a cooling age. Coincidentally in the case of D_2, the final age is within 1 Ma of the deformation age but this is simply because we have chosen to look at deformation taking place at T_c. The same cooling age is observed for deformation at D_3. Consequently, for the case where there is no change in grain size and no resetting of isotope systems by the active deformation mechanisms, no deformation age can be obtained.

4.2. Deformation-induced neocrystallisation

In our next example, we assume that deformation is associated with neocrystallisation and that these new grains have a final grain radius of 1 mm. In the case of D_1, our results are identical to a previous example and the final age will be a cooling age. In the case of D_2, the new grains grown at their closure temperature will undergo the loss of some radiogenic argon component during the early stages of cooling. Modelling (not shown here) shows the difference between the real deformation age and the apparent grain ages to be of the order of 1 Ma. The exact figure has a grain size dependence and would change if we were to consider growing different size new grains at a different temperature (but still at their closure temperature). In the case of D_3, where deformation and grain growth has occurred 50°C below T_c (Fig. 4b), only the outermost 0.2 mm of the grain undergoes any argon loss after the deformation event [Fig. 4b(i)]. The final age is a close approximation to the age of deformation [Fig. 4b(ii)]. In this scenario of new grain growth, it is important to emphasise that an age approaching the deformation age will only be obtained when deformation (i.e. neocrystallisation) occurs below the closure temperature of the grains that are growing during the deformation. Furthermore, the magnitude of the discrepancy between the deformation age and the apparent age [Fig. 4b(ii)] will be controlled by the difference between
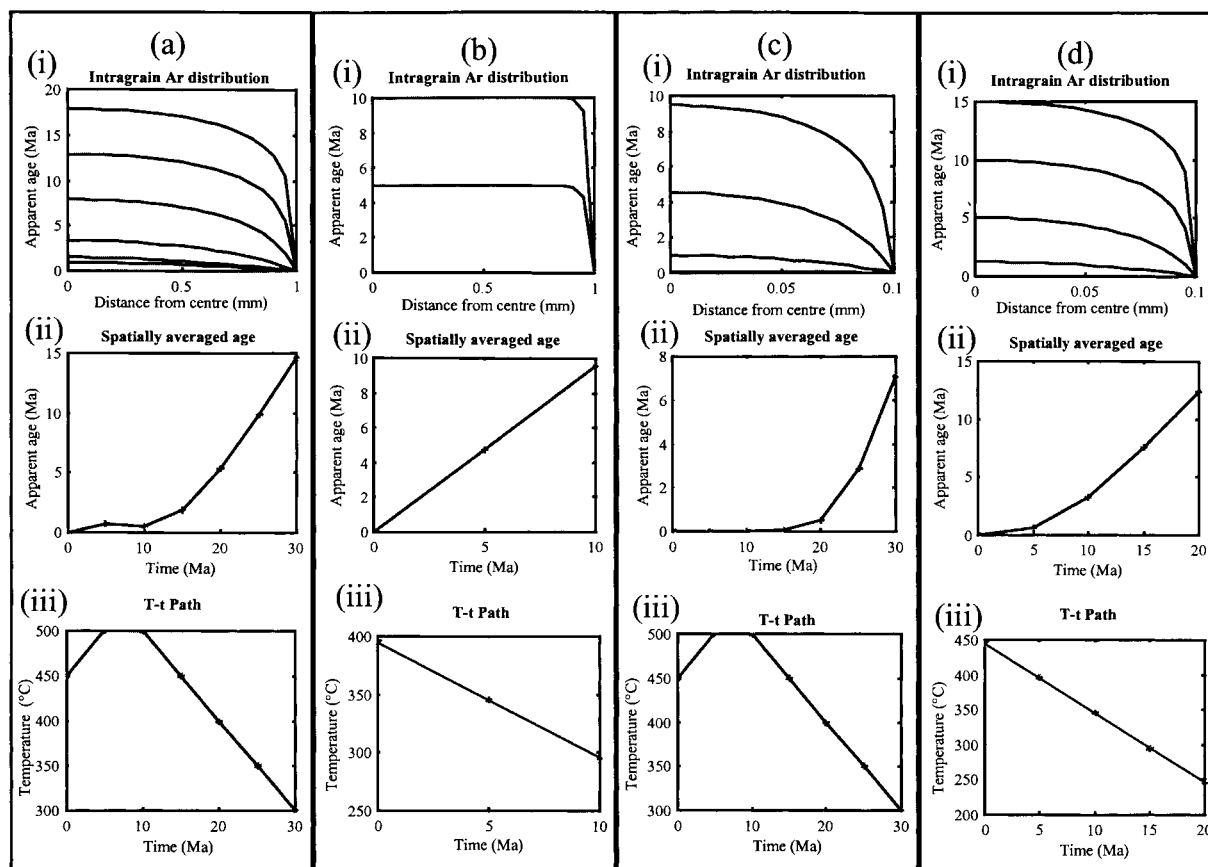
Fig. 4. Selection of diffusion models used to investigate the relationships between deformation and argon isotope systematics with temperature and time. In cases a–d the three graphs (i–iii) illustrate the relationship between apparent argon ages across the grain (i) and how the bulk age of the grain evolves with time (ii). Lines in (i) correspond to the crosses marked on the age-time line (ii) and temperature–time path (iii). In each individual case (a–d) deformation took place at $t = 0$. The time axes in (ii) and (iii) therefore mark the true time since deformation. The discrepancy between the true age and the obtained argon age is given by the difference in this age and the apparent ages shown in (i) and (ii). (a) Argon distribution for a 1 mm grain deformed at D_1 on the prograde part of the T–t curve. (b) Argon distribution for a 1 mm newly crystallised grain that grew during D_3. (c) Argon distribution for a grain, reduced by deformation to 0.1 mm during D_1. Comparison with (a) illustrates the effect of a reduced T_c. (d) Effect of grain size reduction and isotopic resetting during deformation at D_2 [at T_c of the original 1 mm grains (445°C)]. The final age is a cooling age recording passage through c. 368°C. See text for details.

T_c and the temperature at which the deformation takes place.

The above models of neocrystallisation are clearly an oversimplification. Dynamic crystallisation of new mica grains is likely to produce a range of grain sizes that may be contaminated by relict pre-deformational micas of a different age. However, careful analysis of mica microstructure and grain size distributions prior to argon analysis may allow these complications to be accounted for. This has recently been illustrated by a detailed study of neocrystallisation of white mica during deformation (Dunlap, 1997).

4.3. Deformation associated with a change in grain size

Again, we consider three deformation events taking place at different parts of the T–t path (Fig. 3), but now we consider the effects of grain size changes during deformation. We have modelled the effects of grain radius reduction from 1 mm to 0.1 mm. As outlined earlier both plastic and brittle deformation mechanisms can lead to grain size reduction. However, we can distinguish two different scenarios; firstly deformation in which the mechanism itself does not give rise to isotopic re-equilibration (e.g. cataclasis, Fig. 2m) and secondly mechanisms in which the isotope systematics are reset (e.g. dynamic recrystallisation processes such as grain boundary migration recrystallisation).

For the case of a prograde deformation event (D_1) with a temperature significantly below the thermal peak, both types of mechanism will result in cooling ages. The final age of the sample will date the time at which the sample passes through the closure temperature of the reduced grain size (368°C) not the original grain size [Fig. 4c(i–iii)]. All of the radiogenic argon

produced within the grain is lost by diffusion during the metamorphic peak and the start of argon accumulation takes place 15 Ma after the deformation event. This contrasts with the earlier prograde example (Fig. 4a) where the rate of argon diffusion across the larger grain was sufficiently slow to preserve a small apparent age in the core of the grain. The reduction in grain size in this example changes the time of closure, compared to the 1 mm grain of Fig. 4a, by *c*. 8 Ma. The discrepancy between the deformation age and the argon age would be *c*. 23 Ma.

For deformation around the original closure temperature of the 1 mm grains (D_2), the decrease in grain size significantly reduces T_c and opens all of the grains to isotopic diffusion. Analysis of deformed white micas will again yield cooling ages that correspond to the closure temperature for the 0.1 mm grains.

For D_3, the interpretation of whether the reduced grains yield deformation or cooling ages will depend upon the temperature of the deformation and T_c of the deformed grains. If the temperature of deformation is higher than T_c for the 0.1 mm grains (368°C), the grains will be reset and will record a cooling age. If T_c of the 0.1 mm grains (368°C) is significantly higher than the temperature during deformation then there is a further complication. We must consider whether the deformation mechanism producing the grain size reduction isotopically resets the grain or not. In the case where T_c of the 0.1 mm grains is higher than the temperature of deformation and deformation mechanisms reset the grains isotopically then the measured age will be a deformation age. Where the deformation mechanism does not reset the grain, the radiogenic argon accumulated between original closure of the 1 mm grain and the time of deformation will contribute to the measured age. The measured age will also contain an argon component derived radiogenically since the deformation. Thus, the age will be a mixing age that is older than the true deformation age.

The above examples consider an extremely simple model of grain size reduction. In nature, mixed populations of porphyroclast and recrystallised grains are commonly found (Lister and Snoke, 1984). In such a case (e.g. Fig. 2i) there would be at least two different values for T_c in the same original grain. The reduced grain size at the edge of the original grain would be expected to have lower values of T_c than the porphyroclast core and the cores would be expected to have a lower T_c than the original grain. If we consider this model at D_2, that is at the closure temperature of the original 1 mm grain, then the porphyroclastic cores and the recrystallised grains would have a closure temperature below the temperature of D_2 deformation. The range of grain sizes preserved in different porphyroclastic cores and recrystallised grains would therefore potentially record a range of cooling ages. This can

have advantages. For example, Reddy et al. (1996) illustrated an example of heterogeneous grain size reduction (in biotite) at deformation temperatures significantly above the closure temperature for the observed grain sizes (equivalent to model D_1 or D_2). Although estimates of the age of deformation responsible for the reduction are precluded by this relationship, analysis of different grain sizes yielded important constraints on the post-metamorphic thermal history of the sample. By comparison with the previously discussed models, more complex scenarios can be envisaged in which the range of grain sizes produced during deformation have a range of closure temperatures that vary in such a way with the temperature of deformation that some grains yield cooling ages while others date the deformation.

As well as producing grain size reduction, deformation may cause grain coarsening. Deformation mechanisms such as closed-system diffusive mass transfer (Fig. 2f) may lead to increased grain or effective grain radii and, therefore, an increase in closure temperatures. In some cases, grain coarsening may increase the closure temperature of the mineral to temperatures in excess of the deformation temperature. In this situation, the deformed grains pass from isotopically open to closed systems and will therefore record deformation ages. In the simple thermal model described above, if recrystallised grains are sufficiently coarse that their T_c are greater than the temperature of D_1, the peak temperature and the deformation temperatures of D_2 and D_3, it would be theoretically possible to obtain deformation ages for all three deformation events. Grain coarsening during deformation is, therefore, a potentially powerful tool for dating deformation.

5. Application of ^{40}Ar/^{39}Ar techniques to dating deformation

The above discussion outlines some of the general issues regarding the interpretation of deformation ages. In this section, we specifically discuss the ^{40}Ar/^{39}Ar dating technique and in particular illustrate some of the potential problems of applying the technique to the dating of deformation. We have outlined in the previous sections that to correctly interpret deformation ages a detailed microstructural description of the sample is required. This description should include accurate grain sizes and evidence of the operation of deformation mechanisms and inferences concerning grain size changes if they have occurred. These data must then be used to calculate predicted closure temperatures and these in turn compared to the temperature during deformation. To calculate T_c, the cooling rate and the diffusion parameters for the

system are required. Cooling rates in metamorphic rocks are usually obtained by calculating the closure temperatures of a range of different minerals by a range of different isotope techniques—a somewhat circular argument. Alternative approaches that establish the T–t history of a sample by modelling K-feldspar

Ar data and then use this to constrain the significance of white mica ages (e.g. Dunlap, 1997) are useful. However, the application of K-feldspar modelling to deformed K-feldspar has its own problems (Reddy et al., 1999b). A further complication is that the diffusion parameters for argon diffusion in muscovite are not
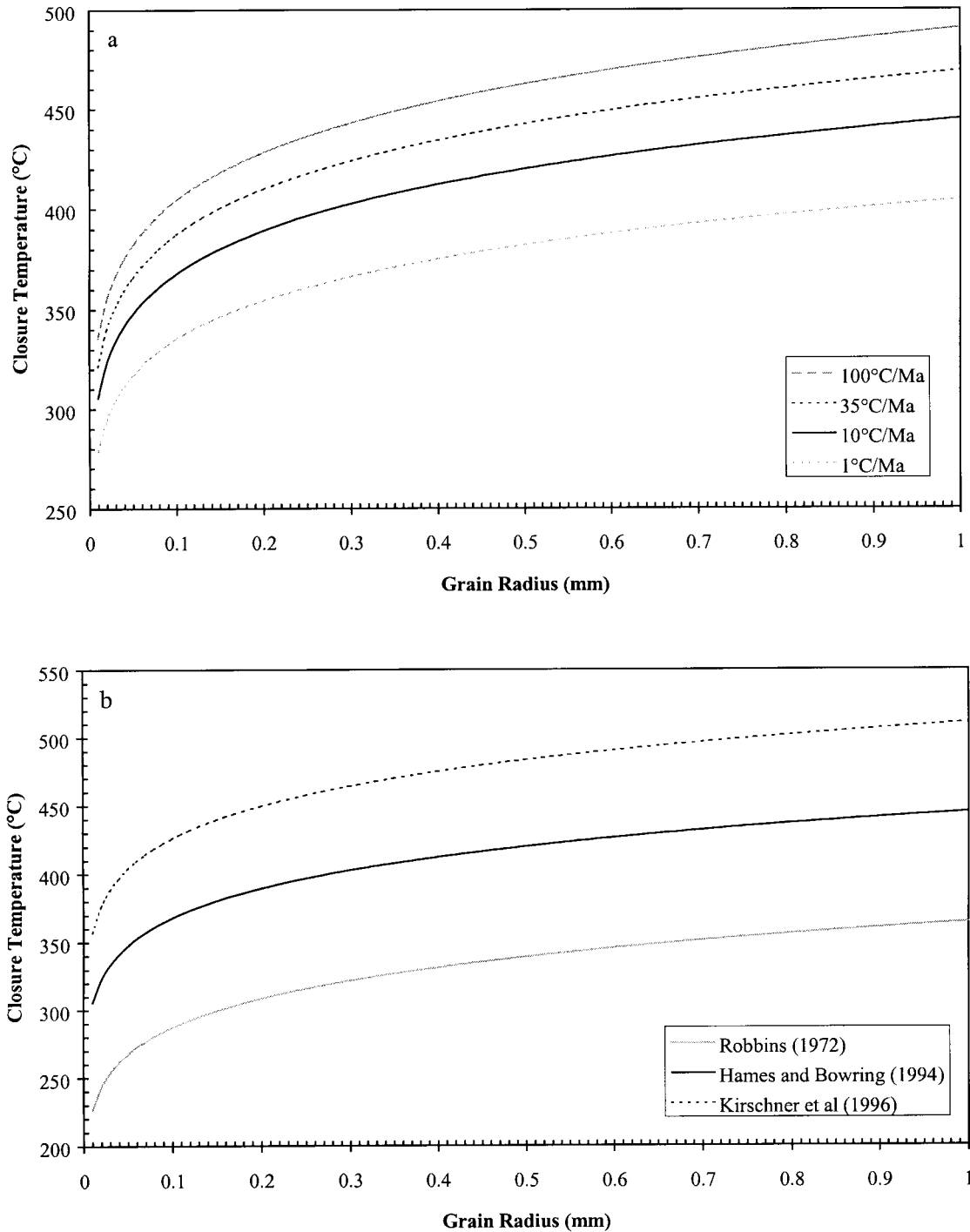

Fig. 5. Illustration of the variation of closure temperature as a function of grain radius for (a) different cooling rates and (b) different diffusion parameters. Detailed microstructural studies may yield well-constrained values for grain radius but large errors in T_c may arise from incorrect selection of cooling rate and diffusion parameters.

well known. Consequently, the estimates of T_c for a particular grain size and cooling rate may be erroneous depending upon which set of preferred parameters are used in the calculation. Indeed, as clearly illustrated by Dunlap (1997), application of incorrect diffusion parameters can lead to completely different interpretations of isotopic data. The likely errors in T_c due to incorrect selection of both cooling rate and diffusion parameters are indicated in Fig. 5. Clearly, for a particular grain size, estimates of T_c may vary considerably. However, as discussed earlier using a correct T_c is paramount to the correct interpretation of deformation ages. There is, therefore, an urgent need for further research to better constrain these diffusion parameters.

6. Conclusions

The temperature control on diffusion is strongly linked to grain size and therefore processes that may modify grain size may modify isotope systematics. A range of deformation mechanisms may take place in micas. These have different implications for grain size modification and the resetting of isotope systems during deformation. To utilise the relationship between deformation and isotope diffusion and interpret deformation ages requires a full understanding of the potential interactions of these mechanisms and the thermal history of the sample. For argon diffusion in micas, diffusional anisotropy suggests there will also be a relationship between grain orientation and age. Our results from simple modelling illustrate that in deforming rocks in which there is no change in grain size, it is difficult to get true deformation ages. In the cases where deformation causes a change in grain size, it is important to characterise the temperature of deformation and the closure temperature of grains formed during the deformation. Without this information, distinction between cooling and deformation ages is equivocal. The development of grains with T_c greater than the temperature during deformation will record a deformation age. This situation may arise in the following cases; (i) neocrystallisation, (ii) when grain size reduction occurs at temperatures below T_c of the reduced grain size and the deformation mechanism has reset the grains; (iii) when deformation-induced grain coarsening has occurred. Since closure temperatures are also dependent upon cooling rate and diffusion parameters, these must also be known for a correct interpretation of the radiometric data.

Acknowledgements

References

Behrmann, J.H., 1984. A study of white mica microstructure and microchemistry in a low grade mylonite. Journal of Structural Geology 6, 283–292.

Bell, I.A., Wilson, C.J.L., 1981. Deformation of biotite and muscovite: TEM microstructure and deformation model. Tectonophysics 78, 201–228.

Bell, I.A., Wilson, C.J.L., McLaren, A.C., Etheridge, M.A., 1986. Kinks in mica: Role of dislocations and (001) cleavage. Tectonophysics 127, 49–65.

Bell, T.H., 1979. The deformation and recrystallisation of biotite in the Woodroffe Thrust Mylonite Zone. Tectonophysics 58, 139–158.

Bell, T.H., Rubenach, M.J., 1983. Sequential porphyroblast growth and crenulation cleavage development during progressive deformation. Tectonophysics 92, 171–194.

Christofferson, R., Kronenberg, A.K., 1993. Dislocation interactions in experimentally deformed biotite. Journal of Structural Geology 15, 1077–1095.

Cosgrove, J.W., 1976. The formation of crenulation cleavage. Journal of the Geological Society of London 132, 155–178.

Dodson, M.H., 1973. Closure temperature in cooling geochronological and petrological systems. Contributions to Mineralogy and Petrology 40, 259–274.

Dodson, M.H., 1986. Closure profiles in cooling systems. Materials Science Forum 7, 145–153.

Dunlap, W.J., 1997. Neocrystallisation or cooling? ^{40}Ar/^{39}Ar ages of white micas from low-grade mylonites. Chemical Geology 143, 181–203.

Dunlap, W.J., Teyssier, C., McDougall, I., Baldwin, S., 1991. Ages of deformation from ^{40}Ar/^{39}Ar dating of white micas. Geology 19, 1213–1216.

Eisbacher, G.H., 1970. Deformation mechanics of mylonitic rocks and fractured granites in Cobequid Mountains, Nova Scotia, Canada. Geological Society of America Bulletin 81, 2009–2020.

Etheridge, M.A., Hobbs, B.E., 1974. Chemical and deformational controls on recrystallization of mica. Contributions to Mineralogy and Petrology 43, 111–124.

Freeman, S.R., Inger, S., Butler, R.W.H., Cliff, R.A., 1997. Dating deformation using Rb–Sr in white mica: Greenschist facies deformation ages from the Entrelor shear zone, Italian Alps. Tectonics 16, 57–76.

Gibson, R.G., 1990. Nucleation and growth of retrograde shear zones: an example from the Needle Mountains, Colorado, USA. Journal of Structural Geology 12, 339–350.

Giletti, B.J., 1974. Studies in diffusion, I. Argon in phlogopite mica. In: Hofmann, A.W., Giletti, B.J., Yoder, H.S., Yund, R.A. (Eds.), Geochemical Transport and Kinetics. Carnegie Institution of Washington, pp. 107–115.

Goodwin, L.B., Renne, P.R., 1991. Effects of progressive mylonitization on Ar retention in biotites from the Santa Rosa mylonite zone, California, and thermochronologic implications. Contributions to Mineralogy and Petrology 108, 283–297.

Goodwin, L.B., Wenk, H.-R., 1990. Intracrystalline folding and cataclasis in biotite of the Santa Rosa mylonite zone: HVEM and TEM observations. Tectonophysics 172, 201–214.

Hames, W.E., Bowring, S.A., 1994. An empirical evaluation of the

argon diffusion geometry in muscovite. Earth and Planetary Science Letters 124, 161–167.

Kanaori, Y., Kawakami, S.-I., Yairi, K., 1991. Microstructure of deformed biotite defining foliation in cataclasite zones in granite, central Japan. Journal of Structural Geology 13, 777–785.

Kelley, S.P., 1988. The relationship between K–Ar mineral ages, mica grain sizes and movement on the Moine Thrust Zone, NW Highlands, Scotland. Journal of the Geological Society of London 145, 1–10.

Kelley, S.P., Reddy, S.M., Maddock, R., 1994. Laser-probe ^{40}Ar/^{39}Ar investigation of a pseudotachylyte and its host rock from the Outer Isles thrust, Scotland. Geology 22, 443–446.

Kirschner, D.L., Cosca, M.A., Masson, H., Hunziker, J.C., 1996. Staircase ^{40}Ar/^{39}Ar spectra of fine-grained white mica—timing and duration of deformation and empirical constraints on argon diffusion. Geology 24, 747–750.

Kligfield, R., Hunziker, J., Dallmeyer, R.D., Schamel, S., 1986. Dating of deformation phases using K–Ar and ^{40}Ar/^{39}Ar techniques: results from the Northern Apennines. Journal of Structural Geology 8, 781–798.

Kralik, M., Klima, K., Riedmüller, G., 1987. Dating fault gouges. Nature 327, 315–317.

Kronenberg, A.K., Kirby, S.H., Pinkston, J., 1990. Basal slip and mechanical anisotropy of biotite. Journal of Geophysical Research 95, 19257–19278.

Lee, J.K.W., 1995. Multipath diffusion in geochronology. Contributions to Mineralogy and Petrology 120, 60–82.

Lee, J.K.W., Aldama, A.A., 1992. Multipath diffusion: A general numerical model. Computers and Geosciences 5, 531–555.

Li, G., Peacor, D.R., Merriman, R.J., Roberts, B., van der Pluijm, B.A., 1994. TEM and AEM constraints on the origin and significance of chlorite–mica stacks in slates: an example from Central Wales, U.K. Journal of Structural Geology 16, 1139–1157.

Lister, G.S., Snoke, A.W., 1984. *S–C* mylonites. Journal of Structural Geology 6, 617–638.

Mares, V.M., Kronenberg, A.K., 1993. Experimental deformation of muscovite. Journal of Structural Geology 15, 1061–1075.

Meike, A., 1989. In situ deformation of micas: a high-voltage electron-microscope study. American Mineralogist 74, 780–796.

Pickles, C.S., Kelley, S.P., Reddy, S.M., Wheeler, J., 1997. Determinations of high spatial resolution argon isotope variations in metamorphic biotites. Geochimica et Cosmochimica Acta 61, 3809–3824.

Reddy, S.M., Kelley, S.P., Wheeler, J., 1996. A ^{40}Ar/^{39}Ar laserprobe study of rocks from the Sesia Zone: Excess argon, argon loss and implications for metamorphic and deformation histories. Journal of Metamorphic Geology 14, 493–508.

Reddy, S.M., Kelley, S.P., Magennis, L., 1997. A microstructural and argon laserprobe study of shear zone development on the western margin of the Nanga Parbat Syntaxis, north Pakistan. Contributions to Mineralogy and Petrology 128, 16–29.

Reddy, S.M., Wheeler, J., Cliff, R.A., 1999a. The geometry and timing of orogenic extension: An example from the western Italian Alps. Journal of Metamorphic Petrology (in press).

Reddy, S.M., Potts, G.J., Kelley, S.P., 1999b. The effects of deformation-induced microstructures on intragrain argon isotope ages in K-feldspar. Geology 27, 363–366.

Shea, W.T., Kronenberg, A.K., 1992. Rheology and deformation mechanisms of an isotropic mica schist. Journal of Geophysical Research 97, 15201–15237.

Shea, W.T., Kronenberg, A.K., 1993. Strength and anisotropy of foliated rocks with varied mica contents. Journal of Structural Geology 15, 1097–1121.

Thoni, M., 1988. Rb–Sr isotopic resetting in mylonites and pseudotachylites: Implications for the detachment and thrusting of the Austroalpine basement nappes in the Eastern Alps. Jahrbuch der Geologischen Bundesanstalt Wein 131, 169–201.

West, D.P.J., Lux, D.R., 1993. Dating mylonitic deformation by the ^{40}Ar–^{39}Ar method: An example from the Norumbega Fault Zone, Maine. Earth and Planetary Science Letters 120, 221–237.

Wheeler, J., 1996. DIFFARG: A program for simulating argon diffusion profiles in minerals. Computers and Geosciences 22, 919–929.

Wijbrans, J.R., McDougall, I., 1986. ^{40}Ar/^{39}Ar dating of white micas from an Alpine high-pressure metamorphic belt on Naxos (Greece)—the resetting of the argon isotopic system. Contributions to Mineralogy and Petrology 93, 187–194.

Wilson, C.J.L., Bell, I.A., 1979. Deformation of biotite and muscovite: Optical microstructure. Tectonophysics 58, 179–200.

Worley, B., Powell, R., Wilson, C.J.L., 1997. Crenulation cleavage formation: Evolving diffusion, deformation and equilibration mechanisms with increasing metamorphic grade. Journal of Structural Geology 19, 1121–1135.